16th World Conference on Earthquake, 16WCEE 2017
Santiago Chile, January 9th to 13th 2017
Paper N° 737
Registration Code: S-D1461872434

CONSTANT YIELD DISPLACEMENT APPROACH FOR SEISMIC DESIGN OF STRUCTURES

A. Tsiavos[(1)], B. Stojadinovic[(2)]

[(1)] PhD Candidate, ETH, Zurich, Stefano-Franscini-Platz 5, 8093, tsiavos@ibk.baug.ethz.ch

[(2)] Professor, ETH Zurich, Stefano-Franscini-Platz 5, 8093, stojadinovic@ibk.baug.ethz.ch

Abstract

The existing relations between the vibration period, the strength reduction factor and the ductility demand of stiff fixed-base structures indicate that these structures should not be allowed to yield (i.e. Ry=1). This design approach is based on the argument that the inelastic ductility demand of these structures, if they were allowed to yield, would be very high.

This study shows that these ductility demand values are not realistic: they emerge from the constant-period, forced-based design methodology, which leads to unrealistically small yield displacement estimates.

Further, this study quantifies the relation between the strength and deformability of structures, based on the argument that the yield displacement of a structure in bending depends mainly on the yield strain of the yielding material and the geometry of the structure and that it does not dependent strongly on the bending strength of that structure. This relation is determined through a statistical analysis of the response of a fixed-base single-degree-of-freedom inelastic structure excited by a large number of recorded ground motions. These motions cover a wide range of ground motion types, magnitudes and distances.

Based on this relation, a new seismic design approach is proposed, the Constant-Yield-Displacement-Design (CYDD) approach. This approach is based on the independence of the strength and the yield displacement of a structure. Compared to the existing approaches, it offers: 1) a more realistic calculation of the inelastic displacement ductility demand of structures with a predetermined strength; and 2) a more exact determination of the strength that is required to satisfy certain performance objectives expressed in terms of flexural displacement ductility. The vibration period (i.e. stiffness) of the structure does not play a role in the CYDD approach. The four steps of the approach are easy to implement as they are based on existing design practices.

Keywords: Performance-based design, Yield displacement, Yield point spectrum, Seismic design approach

1. Introduction

The inelastic seismic displacement demand for fixed-base structures has been widely investigated by many researchers in the past. The coefficient that has been extensively used to quantify the inelastic displacement demand for single degree of freedom (SDOF) systems is the displacement ductility ratio μ, which is defined as:

$$\mu = \frac{u_{m,s}}{u_{y,s}} \quad (1)$$

where $u_{m,s}$ and $u_{y,s}$ are denoted as the maximum inelastic displacement and the yield displacement of the SDOF system, respectively. The yield strength reduction factor R_y is the ratio of the minimum strength required to maintain the SDOF system response in the elastic range, $F_{el,s}$ and the SDOF system yield strength $F_{y,s}$:

$$R_y = \frac{F_{el,s}}{F_{y,s}} \quad (2)$$

The elastic vibration period of the SDOF system is T_n.

Numerous previous studies have investigated relationships between R_y, μ and T_n for fixed base structures. Newmark and Hall [1], Lai and Biggs [2] and Riddel and Newmark [3] proposed piece-wise linear R_y-μ-T_n relations for fixed-base structures. Riddel, Hidalgo and Cruz [4] and Vidic, Fajfar and Fischinger [5] presented bilinear approximations for R_y-μ-T_n relations. Elgadamsi and Mohraz [6], Arias and Hidalgo [7], Nassar and Krawinkler [8], Miranda [9], and Miranda and Bertero [10] suggested continous nonlinear R_y-μ-T_n functions. According to these studies, the seismic response of structures is categorized in three regions: 1) an "Elastic" or "Acceleration sensitive region", which governs the behavior of very stiff structures; 2) a "Hysteretic energy conservation region"; and 3) a "Displacement conservation region", which is observed for very soft structures.

All these studies were based on the simplifying assumption that the inelastic vibration period of the structure is the same as the elastic one. This constant-period approach is advantageous in terms of calculation simplicity, but it does not consistentlty account for the relation between the stiffness, the strength and the displacement of the SDOF system.

Following the constant-period approach, the yielding displacement of the SDOF system is a linear function of its strength (Eq. 3).

$$u_{y,s} = \frac{F_{el,s}}{k_s \cdot R_y} \quad (3)$$

where k_s is the elastic stiffness of the structure. Consequently, the yield displacements of stiff, low-strength SDOF systems (high k_n and R_y values) calculated using the constant-period approach are very small. Therefore, the ductility demands for such SDOF systems, computed using Eq. 1, are very high even if the inelastic displacements are relatively small. However, the yield displacement of a SDOF structure that respondes by bending depends mainly on the yield strain of the yielding material and the geometry of the structure, i.e. its height and cross-section dimentions, and it does not dependent strongly on the bending strength of that structure [11-17]. Therefore, it can be assumed as constant during the seismic design process.

The goal of this study is to relate the strength and the deformability of SDOF structures yielding in flexure, assuming that the yield displacement of such structures depends only on their geometry and the mechanical characteristics of the yielding material and that it is not affected by the strength of the structure. This relation is used to develp the Constant-Yield-Displacement-Design (CYDD) method for inelastic displacement-based seismic design of structures.

2. Dynamic modelling

The dynamics of a fixed-base structure can be investigated by using a simple single-degree-of-freedom system shown in Fig. 1. Mass m_s represents the mass of the structure. Its elastic stiffness and damping coefficient are denoted as k_s and c_s, while its post-yield stiffness is defiened using coefficient α_s. Displacement u_s of the mass of the structure is measured with respect to the ground. The geometry of the structure is also shown in Fig. 1, with A denoting the symmetrically positioned areas of the cross-section flanges assuming a typical steel I-shape cross section or the areas of the steel reinforcement for a typical concrete or masonry cross section. Treatment of structures with asymmetric sections is analogous but somewhat more involved.

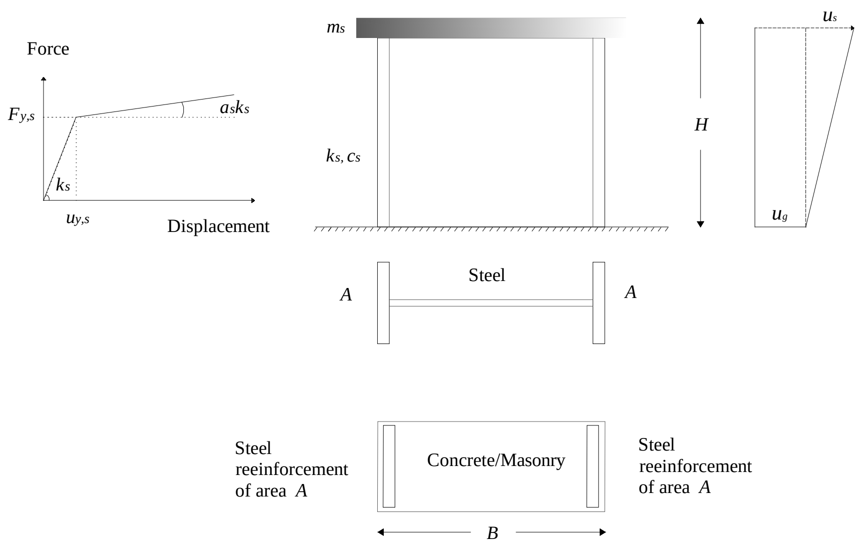

Fig. 1: Parameters of the SDOF model of a fixed-base structure.

Assuming that the SDOF structure responds to the applied ground motion excitation purely in flexure, the following quantities are defined:

1. Yield cross-section curvature $\varphi_{y,s}$:

$$\varphi_{y,s} = \begin{Bmatrix} \dfrac{2\varepsilon_{y,s}}{B} \\ \dfrac{2.1\varepsilon_{y,s}}{B} \end{Bmatrix} \quad \begin{matrix} \text{for steel and concrete sections} \\ \text{for masonry sections [18]} \end{matrix} \tag{4}$$

where $\varepsilon_{y,s}$ is the yield strain of steel.

2. Yield displacement $u_{y,s}$:

$$\mathrm{u}_{y,s} = \frac{1}{3}\varphi_{y,s}H^2 = \frac{1}{3}\frac{2\varepsilon_{y,s}}{B}H^2 = \frac{2}{3}\varepsilon_{y,s}\frac{H^2}{B} \tag{5}$$

assuming the error made for massonry sections is negligibly small.

3. Yield strength reduction factor R^*, as shown in Fig. 2, where $F^*_{el,s}=F_{el,s}$ is the strength of the SDOF structures with a given yield displacement $u_{y,s}$ required for it to remain elastic under a given ground motion excitation and $F^*_{y,s}$ is the yield strength of the structure with the same yield displacement $u_{y,s}$. Note here the assumption that the yield displacement of the SDOF structure remains the same regardless of its strength.

$$R^* = \frac{F^*_{el,s}}{F^*_{y,s}} \tag{6}$$

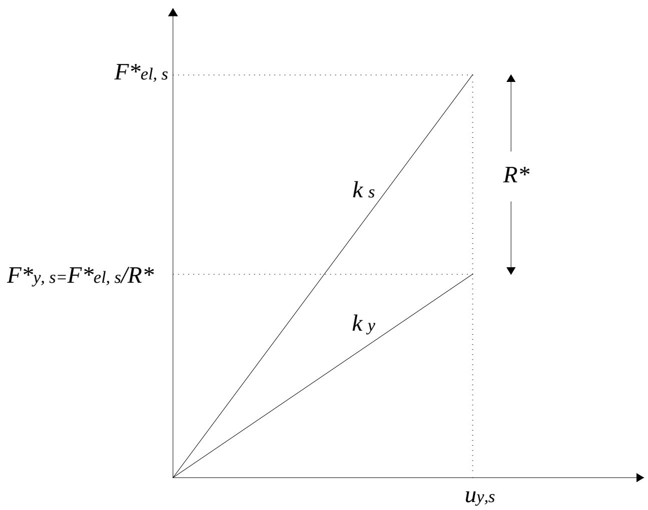

Fig. 2: Definition of the yield strength reduction factor R*

Comentario [BSt1]: Technically, the distance shown is (R*-1)F*ys

Maybe be best to write F*ys = F*els/R*

4. Yield stiffness k_y, corresponding to the yield displacement:

$$k_y = \frac{k_s}{R^*} \tag{7}$$

5. Yield strength of the structure is:

$$F^*_{y,s} = k_y u_{y,s} \tag{8}$$

6. Elastic period and cyclic frequency:

$$T_n = 2\pi\sqrt{\frac{m_s}{k_s}} = 2\pi\sqrt{\frac{m_s}{F_{el,s}/u_{y,s}}} \qquad \omega_n = 2\pi\sqrt{\frac{k_s}{m_s}} = 2\pi\sqrt{\frac{F_{el,s}/u_{y,s}}{m_s}} \tag{9}$$

7. Yield period and cyclic frequency, corresponding to the yield displacement:

$$T_y = 2\pi\sqrt{\frac{m_s}{k_y}} = 2\pi\sqrt{\frac{m_s}{F_{el,s}/(R^* u_{y,s})}} \qquad \omega_n = 2\pi\sqrt{\frac{k_y}{m_s}} = 2\pi\sqrt{\frac{F_{el,s}/(R^* u_{y,s})}{m_s}} \tag{10}$$

A Bouc-Wen [19] model in parallel with a viscous damper with damping coefficient c_s is used to represent the bilinear hysteretic behavior of the SDOF structure, as was done in [20, 21, 22]. The restoring force of the structure with stiffness k_y is given by:

$$F_s(t) = -a_s k_y u_s(t) - (1-a_s) k_y u_{y,s} z_s(t) - c_s \dot{u}_s(t) \tag{11}$$

where z_s is an internal variable of the Bouc-Wen model given by the evolution equation

$$\dot{z}_s(t) = \frac{1}{u_{y,s}}\left(\dot{u}_s(t) - \gamma_{BW}\left|\dot{u}_s(t)\right| z_s(t)\left|z_s(t)\right|^{n-1} - \beta \dot{u}_s(t)\left|z_s(t)\right|^{n}\right), \tag{12}$$

where β, γ_{BW} and n are dimensionless quantities that control the hysteretic behavior of the model. Parameters β and γ_{BW} are set equal to 0.5 and n is set equal to 50 to obtain a sharp transition from the first to the second slope of the SDOF system force-deformation response envelope. The resulting hysteresis is elastic-plastic without pinching.

Dynamic equilibrium of the structure with stiffness k_y and strength $F_{y,s}$ (Fig. 2) gives:

$$a_s k_y u_s + (1-a_s) k_y u_{y,s} z_s + c_s \dot{u}_s = -m_s(\ddot{u}_g + \ddot{u}_s) \tag{13}$$

From Eq. (7):

$$a_s k_s u_s / R^* + (1-a_s) k_s u_{y,s} z_s / R^* + c_s \dot{u}_s = -m_s(\ddot{u}_g + \ddot{u}_s) \tag{14}$$

Eq. (15) is derived by dividing Eq. (14) by m_s:

$$\ddot{u}_s = -a_s k_s u_s / R^* - (1-a_s) k_s u_{y,s} z_s / R^* - c_s \dot{u}_s - \ddot{u}_g \tag{15}$$

The results presented in this study were obtained by solving Eq. (15) using Matlab and Opensees.

3. Dimensional analysis of the seismic response of SDOF structures

An analytical symmetric Ricker pulse (Ricker 1943 [23]):

$$\ddot{u}_g(t) = a_p\left(1 - \frac{2\pi^2 t^2}{T_p^2}\right) e^{\frac{1}{2}\frac{2\pi^2 t^2}{T_p^2}} \tag{16}$$

with a given pulse period T_p and pulse peak acceleration a_p given by Eq. (16) is used to excite the base of a SDOF structure (Figures 1 and 2) and compute its maximum inelastic displacement $u_{m,s}$. This displacement is a function of 7 variables (Eq. 15 and 16):

$$u_{m,s} = f_1(T_n, \alpha_s, u_{y,s}, \xi_s, R^*, a_p, T_p) \tag{17}$$

The yield displacement of the SDOF structure depends on its yielding material and geometry (Eq. 5): it is known once the yield strain, the aspect ratio (H/B) and the height of the structure H are selected.

$$u_{y,s} = f_2\left(\varepsilon_{y,s}, H, \frac{H}{B}\right) \tag{18}$$

The corresponding elastic vibration period T_n of the SDOF structure is determined using the elastic symmetric Ricker pulse ground motion response spectrum as the shortest vibration period that corresponds to the computed SDOF structure yield displacement (Fig. 3). Therefore:

$$T_n = f_3\left(u_{y,s}, a_p, T_p\right) \tag{19}$$

and T_n is not an independent variable in Eq. 17.

The strength of the SDOF structure required for it to remain elastic under the symmetric Ricker pulse ground motion excitation is:

$$F^*_{el,s} = m\left(\frac{2\pi}{T_n}\right)^2 u_{y,s} \tag{20}$$

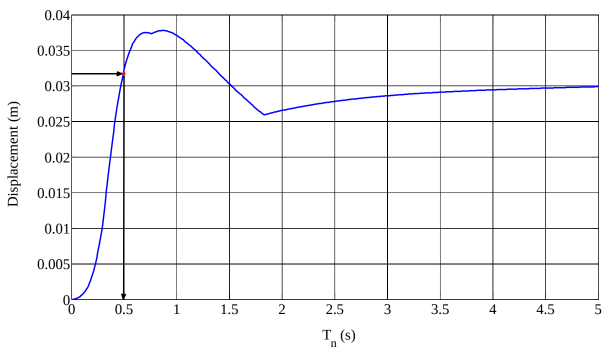

Fig. 3: Determining the elastic vibration period T_n of the SDOF structures that corresponds to the selected value of the yield displacement and the chosen ground motion excitation. The elastic displacement response spectrum shown is for a symmetric Ricker pulse ground motion excitation with T_p= 0.5 s and a_p =0.25 g.

The yield strength of the SDOF structure is then determined using Eq. (6) by selecting the yield strength reduction factor R^*. The yield vibration period T_y is determined using Eq. (10). Finally, the ductility demand for the selected inelastic SDOF structure (with the selected yielding material, height, aspect ratio, yield strength reduction factor, post-yield hardening ratio and non-hysteretic damping ratio under the symmetric Ricker pulse ground motion excitation with a given given pulse period T_p and pulse peak acceleration a_p) is a function of 8 variables:

$$\mu = \frac{u_{m,s}}{u_y} = f_4(\varepsilon_{y,s}, H, \frac{H}{B}, a_s, \xi_s, R^*, a_p, T_p) \tag{21}$$

4. Comparison of the response of a stiff structure to analytical pulse excitation using different seismic design approaches

Consider a prototype SDOF steel structure with aspect ratio H/B=2, H=2 m, mass m_s=1000 tons and non-hysteretic damping ratio ζ=0.02. The yield displacement of this structure is $u_{y,s}$=5.3mm = 0.0053m (Eq. 5). The base of the structure is excited by an analytical symmetric Ricker pulse with a pulse period T_p=0.5s and pulse peak acceleration a_p=0.25g (Eq. 16). The corresponding elastic vibration period T_n=0.22s (Eq. 9, Fig. 3) and the strength of the structure required for it to remain elastic under the given excitation is $F^*_{el,s} = F_{el,s}$ = 3918 kN (Eq. 20). The objective is to evaluate the ductility demand imposed on an SDOF structure whose strength is 4 times smaller than 3918 kN, i.e. $F_{y,s}$ = 979.5 kN.

The inelastic SDOF structure is first designed using the constant-yield-displacment approach, assuming that the yield displacement of the structure remains constant as its strength is reduced. The yield strength reduction factor R^*=4, and the vibration period corresponding to the yield displacement of the structure T_y= 0.46s (Eq. 10). Using Eq. 17 to compute the maximum inelastic displacement of this SDOF structure $u_{m,s}$ = 46.1 mm, the displacement ductility demand is μ=8.7.

Then, another inelastic SDOF system is designed using the conventional constant-period approach. Thus, the period of this inelastic SDOF remains T_n=0.22s. Using a strength reduction factor R_y=4, the yield displacement of the structure $u_{y,s}$=1.2 mm (Eq. 3). Under the same symmetric Ricker pulse motion the maximum inelastic displacement of this SDOF structure is $u_{m,s}$= 37.9 mm (Eq.17), but the resulting displacement ductility demand is μ=31.57, about four times larger than the one calculated for the SDOF structure designed using the constant-yield-displacement approach.

The displacement reponse time history and the force-deformation response of the two inelastic SDOF structures subjected to the selected symmetric Ricker ground motion excitation are shown in Fig. 4. While the maximum inealstic displacements of the two structures are not very different, the computed displacement ductility demand is significantly different. This is because the yield displacement of the structucture imposed by keeping its period constant whule reducing its strength is unreaslistically small. In this case, the yield displacement of 1.2mm would correspond to a H=2m tall structure with an aspect ratio of less than 0.5 (Eq. 5), i.e. a width B of more than 4m, that is unlikely to respond in bending. Altenately, if the structure aspect ratio H/B remains equal to 2 such that its response mechanism remains bending, its height would have to be smaller than 0.5m and width smaller than 0.25m. Such significant changes in response mechanicsm or size of the structure imposed by the constant-period approach are not reasonable. In constrast, the constant-yield-displacment approach produces a reasonable design that preserves the intended response mode and size of the structure.

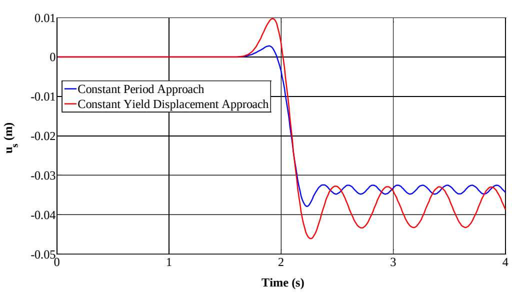

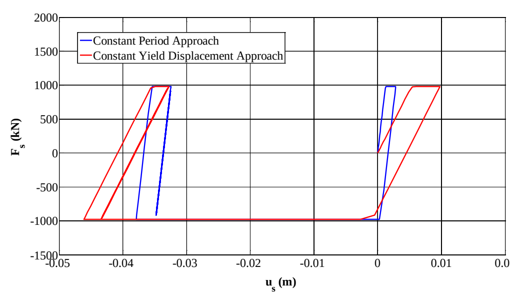

Fig. 4: Displacement time-history response and force-displacement response of the two inealstic SDOF structures to a symmetric Ricker ground motion excitation.

5. Comparison of the yield strength reduction factors R^* and R_y

The yield strength reduction factor R^* proposed in this paper (Eq. 6, Fig. 2) is different from the conventional yield strength reduction factor R_y. The ratio of the two yield strength reduction factors can be easily determined using the elastic pseudo-acceleration response spectrum of the ground motion excitation. For example, take an elastic ground motion design spectrum. Assuming that the yield strength of the SDOF system is $F_{y,s}$, and that the elastic and yield vibration periods T_n and T_y are in the displacement-preserved ranges (larger than corner period T_c such that the elastic design pseudo-acceleration is inversely proportional to the vibration period), the yield strength reduction factor ratio is:

$$\frac{R^*}{R_y} = \frac{\dfrac{F_{el,s}^*}{F_{y,s}}}{\dfrac{F_{el,s}}{F_{y,s}}} = \frac{F_{el,s}^*}{F_{el,s}} = \frac{\dfrac{C}{T_y}}{\dfrac{C}{T_n}} = \frac{T_n}{T_y} \tag{22}$$

From Eq. 9,10:

$$\frac{T_n}{T_y} = \sqrt{R^*} \tag{23}$$

Then, Eq. 22 becomes:

$$\frac{R^*}{R_y} = \sqrt{R^*} \tag{24}$$

Or

$$R^* = \sqrt{R_y} \tag{25}$$

6. Ground motion response data

To further investigate the trend observed in the example above, displacement ductility response spectra of a portfolio of inelastic SDOF structures designed using the constant-yield-displacement approach were computed for an ensemble of recorded ground motions. The yield strength reduction factor R^* was set to 3. The yielding materal of the SDOF structures was steel, with ε_y=0.2% and the and elasticity modulus E=210 GPa and the height H was set to 2m. The portfolio of SDOF structures was created by varying the aspect ratio *H/B* by setting it equal to integers in the set {1,2,…10}. The ensemble comprises 80 motions that cover a wide range of ground motion types, magnitudes (5.5 to 7.7) and distances (10 to 60 km). The motions were obtained from the Pacific Earthquake Engineering Research (PEER) Center next generation attenuation (NGA) strong motion database [24, 25].

The maximum inelastic displacement, and thus the displacemement ductility demand, was computed by conducting a nonlinear time history analysis using Eq. 17 for each SDOF structure and each ground motion. The SDOF structure remained elastic (μ<1) for some aspect ratio values and some ground motions: these cases were taken out of further analysis. Then, for each aspect ratio *H/B* value, the set of displacement ductility values larger than 1 was statistically analyzed: a log-normal distribution was fit to the data and the fit was evaluated using the goodness-of-fit test. The resulting median displacement ductility spectrum, plotted against the *H/B* aspect ratio instead of a vibration period of the SDOF structure, is shown in Fig. 5.

Also shown are the log-normal distribution functions of the displacement ductility data for structures with aspect ratios equal to 1, 5 and 10. Evidently, there are cases when the attained displacement ductility is quite small, meaning that the inelastic SDOF structure deforms less than it would if it was strong enough to remain elastic. The number of such cases grows for larger aspect ratios: for the selected SDOF structure, an aspect ratio of *H/B*>5 corresponds to yield vibration periods larger than 0.5s. A similar trend was observed by Chopra and Chintanapakdee [26] for structures with long elastic vibration periods.

An approximation of the computed displacement ductility spectrum is proposed in Eq. 26 and shown in Fig. 6. The approximation is from above such that the probability that the attained displacement ductility demand for a SDOF structure with a given yield strength reduction factor R^* is larger than that predicted by the approximation is smaller than 50%: in this sense, the approximation is on the safe side. A conventional R^*-μ-*H/B* relation (Eq. 27) is the inverse of Eq. 26.

The principal assumption in the dynamic model used in this study is that it responds purely in flexure. Therefore, the proposed relations between the strength reduction factor R^* and the displacement ductility μ do not apply for structures with small aspect ratios. In fact, Eq. 26 and 27 are not applicable when the aspect ratio *H/B* is smaller than 1. Furthermore, the proposed relations should be used with caution when the aspect ratio is smaller than 2 because, depending on the non-yielding material (steel, concrete, masonry), the interaction between flexure and shear may become significant. Therefore, a dotted line is used to plot the proposed relation for *H/B*<2 in Fig. 7.

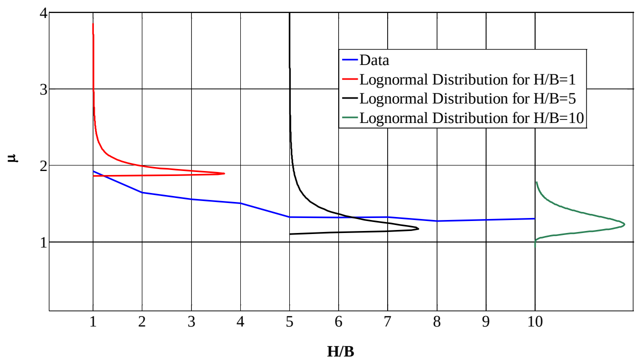

Fig. 5: Median seismic displacement ductility spectrum for SDOF structures designed using the constant-yield-displacement approach with R^*=3 and H=2m and log-normal data distribution functions for aspect ratios equal to 1, 5 and 10

$$\mu=\begin{cases}\text{not applicable} & \frac{H}{B}\leq 1\\ \sqrt{1+\left(R^*-1\right)\frac{(H/B)_c}{\frac{H}{B}}} & 1<\frac{H}{B}\leq (H/B)_c\\ \sqrt{R^*} & \frac{H}{B}>(H/B)_c\end{cases} \tag{26}$$

$$R^*=\begin{cases}\text{not applicable} & \frac{H}{B}\leq 1\\ \frac{\mu^2-1}{(H/B)_c}(H/B)+1 & 1<\frac{H}{B}\leq (H/B)_c\\ \mu^2 & \frac{H}{B}>(H/B)_c\end{cases} \tag{27}$$

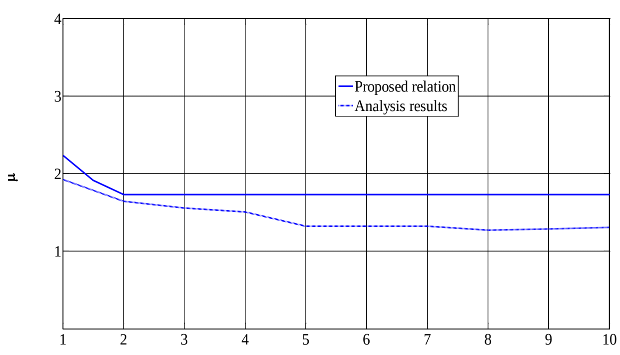

Fig. 6: Median ductility values and proposed values for R^*=3 and H=2m and the proposed μ-R^*-H/B relation (Eq. 26)

The critical aspect ratio value $(H/B)_c$ divides the hyperbolic and constant portions of the μ-R^*-H/B relation proposed in Eq. 26. The transition is governed by the selected yield strain of the yielding material and hardening ratio $\alpha_{,s}$ of the force-deformation response of the SDOF structure (Fig. 1). If steel is the yielding material, then its yield strain depends on its nominal strength. Values of $(H/B)_c$ are shown in Table 2 for SDOF structures with the yield strength reduction factor R^*=4, four typical types of construction steel, three values of the hardening ratio, and three different heights H={1m, 2m, 4m}. Evidently, the hyperbolic region of the proposed μ-R^*-H/B relation becomes smaller for stronger steels (larger yield strain of the yielding material) and stronger post-yield hardening of the SDOF structure force-deformation response. There is, also, a size effect: the hyperbolic region disappears for taller SDOF structures.

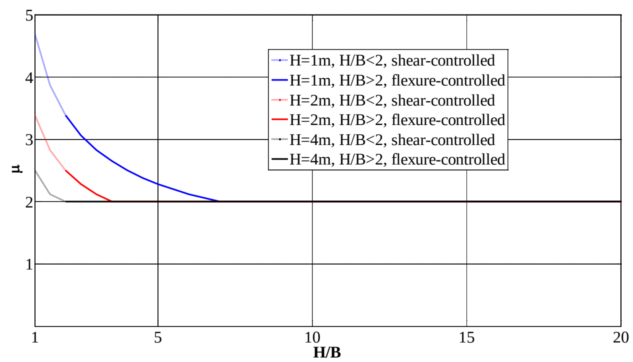

Fig. 7: Proposed μ-R^*-H/B relations for SDOF structuers designed with R^*=4, $\varepsilon_{y,s}$=0.0012 (235MPa steel) and three different SDOF structure heights H = {1,2,4}m.

Table 2: $(H/B)_c$ for different values of α (%) and $\varepsilon_{y,s}$. Height H is entered in meters.

	$(H/B)_c$	α		
$F_{y,s}$	$\varepsilon_{y,s}$	0%	5%	10%
235	0.0012	7m/H	5m/H	5m/H
275	0.0013	5m/H	4m/H	4m/H
355	0.0017	5m/H	4m/H	4m/H
420	0.0020	4m/H	4m/H	4m/H

7. Constant Yield Displacement Design Method

The constant-yield-dispalcement approach was used to develop μ-R^*-H/B and R^*-μ-H/B relations (Eq. 26, 27). These relations can, in turn, be used to implement a Constant-Yield-Displacement Design (CCYD) method for inelastic seismic desing of structures, illustrated in Fig. 8.

Consider a cantilever SDOF structure shown in Fig. 1. First, select its height H, aspect ratio H/B, and yielding material (thus seting the yield strain). Determine the yield displacement in flexure (Eq. 5). Then, based on the anticipated ductility capacity of the structures, compute the maximum inelastic displacement (Eq. 1). Using the elastic design spectrum (plotted in displacement vs. pseudo-acceleration coordinates) for the considered seismic hazard and local soil conditions, determine the strength the SDOF system requires to remain elastic $F^*_{el,s}$. Using the anticipated ductility capacity of the structure μ compute the yield strength reduction factore R^* from the proposed R^*-μ-H/B relation (Eq. 27). Finally, compute the required yield strength of the structures (Eq. 2) and design the area of the yielding material A (Fig.1) accordingly.

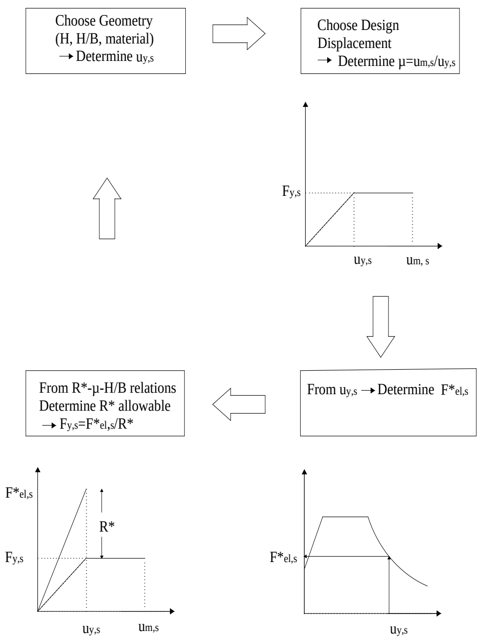

Fig. 8: Steps of the CCYD method

6. Conclusions

This study quantifies the relation between the strength and deformability of structures, based on the argument that their yield displacement is constant and not dependent on their strength. The proposed R^*-μ-H/B relation shows that the inelastic behavior of structures can be categorized in two main regions: First, the short aspect ratio region for structures with short aspect ratios *H/B*, where the ductility demand is significant but not unrealistically high, compared to previous R_y-μ-T_n approaches. Second, the equal-displacement region for structures with higher aspect ratios, where the ductility demand is constant for varying values of the aspect ratio *H/B.* The effect of the increase the strength $F_{y,s}$ on the decrease of the ductility demand of the structure was found to be significant in the short aspect ratio range.

Based on these relation, a new performance-based approach is proposed in this study, the Constant-Yield-Displacement-Design (CYDD) approach. This approach is based on the independence of the strength of the structure on the yield displacement, allowing for: First, more realistic calculations of the inelastic ductility demand of structures with a predetermined strength. Second, more exact determination of the strength that is required to satisfy certain performance objectives (Performance-based design). The four design steps of the approach are easy to implement as they are based on existing design practices.

7. References

[1] Newmark NM, Hall WJ (1973): Seismic design criteria for nuclear reactor facilities, *Report 46*, Building Practices for Disaster Mitigation, National Bureau of Standards, pp. 209–236.

[2] Lai S-SP, Biggs JM (1980): Inelastic response spectra for aseismic building design, J. struct. diu. ASCE **106**

[3] Riddell R, Newmark NM (1979): Statistical analysis of the response of nonlinear systems subjected to earthquakes. Structural Research Series No. 468, Civil Engineering Studies, University of Illinois, Urbana-Champaign, IL

[4] Riddell R, Hidalgo PA, Cruz EF (1989): Response modification factors for earthquake resistant design of short period buildings. *Earthquake Spectra*, **5**(3):571–590.

[5] Vidic T, Fajfar P, Fischinger M (1994): Consistent inelastic design spectra: strength and displacement, *Earthquake Engng. Struct. Dyn.* **23**, 502–521

[6] Elghadamsi FE, Mohraz B (1987): Inelastic earthquake spectra. *Earthquake Engng. Struct. Dyn*., **15**: 91–104

[7] Arias A, Hidalgo PA (1990) New Chilean Code for earthquake-resistant design of buildings, *Proc. 4th U.S. earthquake eng., Palm Springs, EERI*, **2**, 927-936

[8] Nassar AA, Krawinkler H (1991) Seismic demands for SDOF and MDOF systems. *Report No. 95, The John A.Blume Earthquake Engineering Center*, Stanford University, Stanford.

[9] Miranda E (1993): Evaluation of site-dependent inelastic seismic design spectra. *Journal of Structural Engineering (ASCE)*, **119**(5), 1319–1338

[10] Miranda E, Bertero VV (1994): Evaluation of strength reduction factors for earthquake resistant design, *Earthquake Spectra*, **10**, 357–379.

[11] Ascheim M, Black EF (2000): Yield point spectra for seismic design and rehabilitation. *Earthquake Spectra*, **16** (2), 317–335.

[12] Ascheim M (2002): Seismic design based on the yield displacement. Earthquake Spectra, **18** (4), 581–600

[13] Priestley MJN (2000): Performance based seismic design, *Proc. 12th World Conference on Earthquake Engineering*, Paper No. 2831, New Zealand

[14] Priestley MJN, Calvi GM, Kowalsky MJ (2000): Direct Displacement-based Seismic Design of Concrete Buildings, *Bulletin of the New Zealand Society for Earthquake Engineering 33(4), 421-444*

[15] Paulay T (2002): An estimation of displacement limits for ductile systems. *Earthquake Engng Struct. Dyn.*, **31**:583–599

[16] Vamvatsikos D, Aschheim M, Kazantzi A (2014): Direct performance-based seismic design: avant-garde and code-compatible approaches, *Proceedings of the 9th International Conference on Structural Dynamics*, *EURODYN 2014*, Porto, Portugal, 30 June - 2 July.

[17] Beyer K, Simonini S, Constantin R, Rutenberg A (2014): Seismic shear distribution among interconnected cantilever walls of different lengths, *Earthquake Engineering and Structural Dynamics*, **43**, 1423-1441

[18] Priestley MJN., Calvi MC, and Kowalsky, MJ (2007): Displacement-Based Seismic Design of Structures IUSS Press, Pavia, , 670 pp.

[19] Wen, YK (1975): Approximate method for nonlinear random vibration, *J. Eng. Mech. Div.*, **101**(4), 389–401.

[20] Tsiavos A, Vassiliou MF., Mackie KR and Stojadinovic B (2013): R-μ-T relationships for seismically isolated structures, *COMPDYN 2013, 4th International Conference on Computational Methods in Structural Dynamics and Earthquake Engineering*, Kos Island, Greece, 12-14 June

[21] Tsiavos A, Vassiliou MF, Mackie KR and Stojadinovic B (2013): Comparison of the inelastic response of base-isolated structures to near-fault and far-fault ground motions, *VEESD 2013, Vienna Congress on Recent Advances in Earthquake Engineering and Structural Dynamics & D-A-CH Tagung, Vienna*, Austria, 28-30 August.

[22] Vassiliou MF, Tsiavos A and Stojadinovic B (2013): Dynamics of Inelastic Base Isolated Structures Subjected to Analytical Pulse Ground Motions, Earthquake Engineering and Structural Dynamics, **42** (14), 2043-2060.

[23] Ricker N (1943): Further developments in the wavelet theory of seismogram structure. *Bulletin of the Seismological Society of America*, **33,** 197-228.

[24] PEER NGA strong motion database (2010): Pacific Earthquake Engineering Research Center, Berkeley, California (http://peer.berkeley.edu/nga/ on 08.09.2014)

[25] Mackie, KR, and Stojadinovic B (2005): Fragility basis for California highway overpass bridge seismic decision-making. *PEER Report No. 2005/02*, Pacific Earthquake Engineering Research Center, University of California, Berkeley

[26] Chopra AK, Chintanapakdee C (2004): Inelastic deformation ratios for design and evaluation of structures: single-degree-of-freedom bilinear systems. *Journal of Structural Engineering (ASCE)*, 130:1309–1319